Title

Lateral Spread Hazard Mapping of Northern Salt Lake Valley, Utah for a M7.0 Scenario Earthquake

Authors(s)

Michael J. Olsen, Steven F. Bartlett, and Barry J. Solomon

Corresponding (first) author:

Michael J. Olsen
c/o Steven F. Bartlett
122 S. Central Campus Dr., Rm. 104
Salt Lake City, Utah 84112
Phone: 801-244-4836
E-mail address: michael.j.olsen@gmail.com

Submission date for review copies: 9/9/05

Submission date for camera-ready copy:

Lateral Spread Hazard Mapping of the Northern Salt Lake Valley, Utah for a M7.0 Scenario Earthquake

Michael J. Olsen,[a] Steven F. Bartlett,[a] M. EERI, and Barry J. Solomon[b]

This paper describes the methodology used to develop a lateral spread displacement hazard map for northern Salt Lake Valley, Utah using a scenario M7.0 earthquake occurring on the Salt Lake City segment of the Wasatch fault. The mapping effort is supported by a substantial amount of geotechnical, geologic and topographic data for the Salt Lake Valley. ArcGIS® routines used this information to perform a site-specific lateral spread analysis using methods developed by Bartlett and Youd (1992) and Youd et al. (2002) at individual borehole locations. These results were subsequently generalized to the mapped geologic units to fully delineate the lateral spread hazard. The proposed approach is an incremental one that shows how to generalize the site-specific Bartlett-Youd lateral spread regression equations to a regional mapping project. The earthquake event for the proposed method can be from a scenario earthquake or from a probabilistic ground motion. In addition, because the hazard map is based on estimates of lateral displacement, it is useful in delineating zones of potential building damage and areas that require further site-specific geotechnical evaluations. Ultimately, we hope that county and state governments will utilize this map and similar maps to better define the liquefaction hazard for future planning and development.

INTRODUCTION

Lateral spreading occurs when a soil liquefies and blocks of intact, surficial soil move downslope or towards a free face during earthquake shaking. Lateral spreading has caused substantial damage during several major earthquakes, and thus, many researchers have

[a] Dept. Civil and Environmental Eng., University of Utah, 122 S. Central Campus Dr., Salt Lake City Utah, 84112.
[b] Utah Geological Survey, 1594 W. North Temple, P.O. Box 146100, Salt Lake City, Utah 84114-6100.

developed empirical, analytical and numerical methods to estimate the amount of horizontal displacement from lateral spreading. Methods have also been developed to map liquefaction hazards on a regional scale and applied to mapping projects nationwide. Liquefaction hazard maps can be broadly classified as: liquefaction susceptibility, liquefaction potential and liquefaction ground failure maps.

The liquefaction susceptibility mapping technique developed by Youd and Perkins (1978) maps the liquefaction hazard solely on the susceptibility of a soil deposit to liquefaction. Liquefaction potential maps improve on this by combining the soil and seismic information to evaluate liquefaction potential using a scenario earthquake or estimates of strong ground motion from probabilistic seismic hazard analyses. Then, liquefaction ground failure maps begin to predict the extent of liquefaction. In the past, a popular method for producing ground failure maps was the Liquefaction Severity Index (LSI) of Youd and Perkins (1987), which provides an estimate of the maximum amount of horizontal ground displacement in gently sloping, highly susceptible deposits as a function of earthquake magnitude and source distance. More recently, researchers have recognized that the thickness, density and fines content of the liquefiable layer and the surrounding topography play significant roles in affecting the amount of horizontal displacement resulting from lateral spread (Hamada et al., 1986; Bartlett and Youd, 1992; O'Rouke and Pease, 1997; Youd et al., 2002; Rosinski et al., 2004).

To partly incorporate these factors, the Liquefaction Potential Index (LPI) has been used as an indicator of liquefaction-induced ground failure potential. The LPI is an aggregated or lumped index, where one minus the factor of safety against liquefaction is weighted by a linear depth function and integrated in the upper 20 m of the profile (Iwasaki et al., 1978). Studies for Japan and California show that surface manifestation of liquefaction is high when the LPI is greater than 5 and that lateral spread is very likely if a static driving force is present for LPI values greater than about 12 to 15 (Toprak and Holzer, 2003).

The LPI can be used as an indicator of potential liquefaction-induced ground failure, but it does not quantify the amount of horizontal displacement expected at a given location, or within a specific geologic unit. In addition, it does not include the influence of topography on lateral spread, which strongly influences the amount of lateral spread displacement (Bartlett and Youd, 2002).

The potential for liquefaction-induced ground failure has become a major concern along the Wasatch Front because of its inherent potential for large earthquakes and a

substantial amount of loose sand and sandy silt deposited in the adjacent valleys. The effort to develop liquefaction hazard maps in Utah began in 1980 when Utah State University received a National Earthquake Hazards Reduction Program (NEHRP) grant to complete a study for Davis County (Anderson et al., 1982). These potential maps were created based on the limited amount of Standard Penetration Test (SPT) data available at that time. The acceleration values to trigger liquefaction of these sites calculated from the data were compared to the predictions of strong ground motion studies performed in 1978. Then, using the available surficial geologic data as constraints, they produced liquefaction triggering hazard maps delineating zones of low, moderate and high liquefaction potential. These maps have been useful to government agencies and consultants, but these maps can benefit greatly from updating based on available higher quality data and analysis techniques.

To improve these maps and better quantify the liquefaction hazard in Salt Lake Valley, Utah, several probabilistic and scenario liquefaction hazard maps are being created based on geotechnical data collected as part of this project. This paper discusses the use of the Bartlett-Youd lateral spreading regression equations (Bartlett and Youd, 1992) with updated regression coefficients developed based on a larger database (Youd et al., 2002) to produce a lateral spread hazard map for a M7.0 scenario earthquake for northern Salt Lake Valley. The Bartlett-Youd lateral spread model was originally developed for site-specific geotechnical evaluations and includes seismic, soil and topographical factors (Bartlett and Youd, 1992). This study shows how this method can be generalized to a regional mapping project where geotechnical data are available to describe the engineering properties of the major geologic units. Utilizing this method allows for a hazard map to be created that will quantify the displacements, and hence, the building damage expected during a seismic event.

SEISMICITY AND FAULTING

The Salt Lake Valley lies in the central Wasatch Front portion of the Intermountain Seismic Belt (ISB), which is undergoing east-west tectonic extension. The ISB is a north-south trending zone of shallow, intraplate seismicity that extends from Montana, through central Utah, into southern Nevada and northern Arizona (Smith and Arabasz, 1991). The Wasatch fault zone is a segmented normal fault that extends along the Wasatch Front from central Utah into southern Idaho. It separates the Basin and Range Province on the west from the Middle Rocky Mountains on the east. Geologic evidence suggests the segments have relatively persistent boundaries between surface ruptures.

The Salt Lake City segment of the Wasatch fault is the primary seismic threat to Salt Lake City. This segment has a north to south trend on the eastern boundary of Salt Lake Valley (Figure 1). It is approximately 46 km long, extending from the Traverse Mountains salient on the south to the Salt Lake salient on the north (Personius and Scott, 1992). The Salt Lake City segment includes the Warm Springs fault along the Salt Lake salient, the East Bench fault near downtown Salt Lake City, the Cottonwood section near the southern range front and the western part of the Fort Canyon fault near the Traverse Mountains salient. The West Valley fault zone is antithetic to the Salt Lake City segment and may or may not be linked to rupture of the Salt Lake City segment (Figure 1).

On average, the Salt Lake City segment ruptures about every 1200 to 1300 years (Lund, 2005) and is capable of M7.0 (Wong et al., 2002). The largest historical earthquake in the Wasatch Front region was the 1934 Hansel Valley M6.6 earthquake generated by the Hansel Valley fault. Also, in 1910, a maximum Modified Mercalli (MM) intensity of VII was felt in downtown Salt Lake City. This event damaged several buildings, shaking plaster from walls and toppling chimneys, but the strong motion was not associated with the Salt Lake City segment. No historical liquefaction or lateral spread has been recorded in Salt Lake Valley, but prehistoric ground failure from liquefaction has been documented by various geotechnical evaluations and foundation investigations (e.g., Osmond et al., 1965; Simon and Bymaster, 1999; Kleinfelder Inc., 1999).

The scenario earthquake used for the lateral spread hazard map in this report is a M7.0 event that includes rupture of the Warm Springs, East Bench and Cottonwood faults (i.e., all sections of the Salt Lake City segment of the Wasatch fault). Co-seismic rupture of the West Valley fault zone was not considered in the scenario earthquake. The scenario earthquake is capable of generating strong motion throughout much of Salt Lake Valley. Figure 2 shows the peak horizontal ground acceleration (pga) values (*g*) in the mapped area (Wong et al., 2002) for the scenario earthquake. These mapped values include soil effects resulting from amplification and/or deamplification of the strong motion. This map was used in our liquefaction triggering analyses, as explained later.

GEOLOGIC SETTING

Salt Lake Valley occupies the one of the easternmost basins of the Basin and Range Province. This province extends from the Wasatch Range in north-central Utah westward to

the Sierra Nevada in eastern California. Salt Lake Valley is filled with a few tens to several hundred meters of lacustrine, alluvial and fluvial deposits derived from the bounding mountain ranges.

Holocene sediments, deposited after the last regression of Lake Bonneville, and Pleistocene Lake Bonneville deposits dominate the surficial geology of Salt Lake Valley. Holocene lacustrine, marsh and alluvial sediments underlie the northern part of the Salt Lake Valley (Figure 1) (Table 1). These mixed deposits include clay, silt, sand, peat, and minor gravel of about 5 to 10 m thickness. The southern and central part of the valley is underlain by Holocene stream alluvium deposited within the Jordan River channel and its flood plain. The stream alluvium consists of sand, silt, and minor clay and gravel and has a maximum thickness of about 5 to 10 m. Also, stream alluvium is found on the eastern side of the valley, where multiple mountain streams exit the steep canyons of the Wasatch Range and flow northwesterly toward the Jordan River and into Great Salt Lake.

Underlying the Holocene sediments are Pleistocene lacustrine deposits of Lake Bonneville. This freshwater lake occupied much of the valley from about 30,000 to 10,000 years before present (Oviatt et al., 1992). Since the last regression of Lake Bonneville, the lake level has remained close to the present level of Great Salt Lake. The total thickness of Lake Bonneville deposits near the I-15 alignment in the central part of the valley is not clearly defined, but is generally greater than about 10 m.

Alluvial and lacustrine sediments of considerable thickness underlie the Lake Bonneville deposits. Estimates of the total thickness of unconsolidated Quaternary deposits in Salt Lake Valley range from approximately 40 m to as much as 600 m (Wong et al., 2002), depending on the proximity to the deepest part of the basin. Below this, semi-consolidated and consolidated sediments extend to a depth of about 2.6 km, below which bedrock is found (Wong et al., 2002).

GEOLOGIC MAPPING

This mapping project combines geologic and geotechnical data to produce the lateral spread hazard map for Salt Lake Valley. It was important to represent the areal extent and depth of each geologic unit as accurately as possible and to obtain representative geotechnical data for as many geologic units as possible. The surficial geologic map of Personius and Scott (1992) was used for the eastern part of the study area and the work of

Biek et al. (2004) for the Magna quadrangle was used for the southwestern corner of the study area. However, the northwestern portion of Salt Lake County has not been mapped recently. For these areas, extrapolations of geologic units from the boundaries of the Personius and Scott (1992) and Biek et al. (2004) maps were used with the mapping by Miller (1980) serving as reference. The compiled map was digitized into a polygon feature class in a geodatabase so that it could be used programmatically in ArcGIS®.

The geologic maps assisted in comparing and inferring geotechnical properties for the various geologic units during the data collection phase. Each layer in the geotechnical database was assigned to a geologic unit, so that variation of soil properties within and between geologic units could be compared. However, there were a few geologic units where geotechnical data were sparse. Nonetheless, this did not prove to be a large hindrance, because the undersampled units are located predominately in areas with a deep groundwater table and thus are not susceptible to liquefaction and lateral spread.

GEOTECHNICAL DATABASE

Geotechnical data were gathered for each of the geologic units to better define their engineering properties. Efforts to develop a geotechnical database for this area began with the creation of the liquefaction potential maps (Anderson et al., 1982). However, the Anderson et al. (1986) hazard map (Figure 3) was based on a modest geotechnical database. Since then, numerous geotechnical investigations have been performed throughout Salt Lake County, including extensive subsurface investigations and Standard Penetration Testing (SPT) for the I-15 Reconstruction Project during 1998 to 2002 (Figure 4). Also, Cone Penetrometer Testing (CPT), Seismic Cone Penetrometer Testing (SCPT) and downhole suspension logging were performed along the I-15 corridor to obtain shear wave velocity (Vs) measurements for seismic hazard studies.

This proposed lateral spread displacement mapping method can be used when there are a reasonable number of boreholes available for each major geologic unit in the study area. A reasonable number of boreholes implies that the sample size is sufficient to infer the distribution of $(N_1)_{60}$ values, fines content and mean grain size of the saturated cohesionless sediments in the mapped unit. The method cannot be applied to areas where there is no or little subsurface geotechnical data. Thus, it is more applicable to urban developed areas, where geotechnical testing has been performed.

The liquefaction triggering and lateral spread analyses were performed based on data obtained from over 600 SPT boreholes. These borings provided $(N_1)_{60}$ values and other important soil properties such as the thickness of saturated, cohesionless layers with $(N_1)_{60}$ values less than 15 (T_{15}), fines content of these layers (F_{15}) and their mean grain size ($D50_{15}$) (Bartlett and Youd, 1992). In addition, CPT data were collected for approximately 400 soundings, but were unfortunately these data were not used for the subsequent triggering and lateral spread analyses because correlations for estimating T_{15}, F_{15}, and $D50_{15}$ from CPT data are not available, but are currently being developed for future mapping efforts. However, CPT data were used in conjunction with borehole logs to assign the $(N_1)_{60}$ values and corresponding soil properties to their respective geologic unit, when nearby CPT data were available.

The data collection efforts utilized several sources to compile an extensive geotechnical database so that the database would be available for the public not only for this analysis but future analyses as well. A substantial amount of this geotechnical data was obtained from the Salt Lake County government from previous site-specific liquefaction studies. Data from the I-15 Reconstruction Project and other highway investigations were provided by the Utah Department of Transportation (UDOT). These data include borehole logs for the older Interstate 80 (I-80) and Interstate 215 (I-215) construction projects. The I-15 Reconstruction Project subsurface data are a very extensive portion of the database. These data were available in electronic format (GINT® database), allowing for a more rapid transfer of data to the ArcGIS® database. In addition, the borehole data used by Anderson et al. (1986) in their previous mapping were obtained from the Utah Geological Survey and were used to fill in gaps where more recent data were unavailable. Some geotechnical consultants also provided data for the mapping effort (Simon and Bymaster, 1999; Kleinfelder Inc., 1999). These data, in combination, allow a reasonable sampling of most geologic units and had sufficient spatial distribution to perform the various analyses. Some geologic units were not as well sampled as others, but these units are in areas where the soil will not liquefy because the groundwater table is very deep, thus the analysis of these units for lateral spread did not need to be performed and the units were assigned a very low lateral spread hazard.

The geotechnical boreholes along I-15 and other transportation corridors generally extended to depths of 15 m, or greater. In other areas, the major source of subsurface data was from Salt Lake County. These county boreholes typically extended to a depth of about 10 m. Although it would be preferable to have slightly deeper boreholes, these 10-m

deep boreholes are usually sufficiently deep so as to identify lateral spread layers. Bartlett and Youd (1992) found that the depth to the lateral spread zone (i.e., depth with the lowest factor of safety against liquefaction) is usually (about 90 percent of the time) located in the upper 10 m of the profile for areas that underwent significant lateral spread.

Because of variability in the quality of the subsurface data from numerous sources, some soil properties were estimated to fill in data gaps. To keep track of estimated properties, a system of data qualifiers was implemented. The data tables include data qualifier fields for important information, ranking the data quality from 1 to 3. A "1" was given to data and supporting information that was recorded in the originating report. A "2" was given to the data that could be reasonably estimated from nearby borehole logs from the originating report. A "3" denoted data that was estimated from another source beyond the originating report. These data qualifiers will be paramount in the future uncertainty analysis that will be performed in conjunction with future probabilistic liquefaction mapping efforts.

Prior to performing the liquefaction triggering and lateral spread analyses, missing values of soil unit weight, fines content (F_{15}) and mean grain size ($D50_{15}$) that could not be filled in using values obtained from a nearby borehole were determined by averaging the soil properties in the database. These averages were calculated from 2261 fines content and 315 mean grain size measurements from laboratory tests in the compiled dataset that received a data quality ranking of "1." (No penetration resistance data were averaged; if these data were missing, the borehole was not entered into the subsurface database). The averaging was first performed using records with the Unified Soil Classification System (USCS) soil type and geologic unit corresponding to the record missing values for soil properties. These values received a data qualifier of "4" to mark them as average values. In the case that no data were available for a specific soil type within a geologic unit, averages for that soil type were calculated using records with the same USCS soil type independent of geologic unit. These values received a data qualifier of "5" to differentiate them. About 70 percent of the F_{15} and 90 percent of the $D50_{15}$ values used in the analyses were obtained from these laboratory measurements.

In addition to penetration resistance and soil properties, shear wave velocity (Vs) data for Salt Lake Valley (Ashland and McDonald, 2003) from approximately 160 sites were collected and entered into the ArcGIS® database. The Vs measurements were averaged over a 30 m interval (VS_{30}) and over a 12 m interval (VS_{12}). The Vs data were used to assign surficial geologic units to ground response units (Ashland and McDonald, 2003) for strong

ground motion studies (Wong et al., 2002). Estimates of VS_{12} are also required by the methodologies that will be used to perform probabilistic liquefaction triggering analyses in a future project.

A groundwater depth map is required to show which layers are saturated and susceptible to liquefaction and to calculate the effective vertical stress profile for the subsequent liquefaction triggering calculations. Unfortunately, a reliable groundwater map did not exist for the project area, nor were there sufficient historical data to accurately model groundwater depths and fluctuations throughout the valley. Such data would be valuable to the study, if available. To compensate for this lack of data in the estimation of groundwater depths in boreholes without groundwater information, the boreholes with recorded groundwater depths were used in the creation of an interpolated groundwater grid (see Figure 5). Because the groundwater table depths recorded in the borehole data were found to be reasonably consistent in the study area, an inverse distance square method produced the best results as compared to results from Kriging and Spline interpolation methods.

The groundwater depths recorded on these geotechnical logs were recorded at different years and seasons; thus, estimates of groundwater depth need to be conservative to account for potential fluctuations that occur with time. Observations in downtown Salt Lake City near the I-15 alignment show a lowering of the water table of about 5 feet since 1998 following 6 years of severe drought. To reflect these observed fluctuations in the liquefaction triggering and lateral spread analyses, the depth to groundwater was decreased by 5 ft from the recorded value in each borehole. In addition, if part of a sand layer was saturated, it was assumed that the entire layer was saturated for the analyses.

LATERAL SPREAD HAZARD MAP

A liquefaction triggering analysis using the M7.0 scenario earthquake, peak ground acceleration values shown in Figure 2 and the liquefaction triggering analysis methods outlined in Youd et al. (2001) preceded the lateral spread calculations for each borehole in the dataset. Soils with a plastic index greater than 7 typically exhibit “clay-like” behavior during seismic events and do not generally liquefy (Boulanger and Idriss, 2004). Such soils were screened from the liquefaction and lateral spread analyses.

The lateral spread hazard map (Figure 6) was divided into hazard zones according to the calculated horizontal displacement (D_H) at each borehole and the surficial geology. Those areas designated as very high hazard zones have soil, seismic and topographical conditions

that could potentially produce maximum D_H values greater than 1 m for the scenario earthquake. High hazard, moderate hazard and low hazard zones have the potential of D_H values between 0.3 to 1.0 m, 0.1 and 0.3 m and 0.0 to 0.1 m, respectively. Areas where no significant lateral spread was predicted are labeled as minimal hazard.

To produce the lateral spread hazard map shown in Figure 6, calculations and statistical analyses were used in combination with the surficial geologic mapping. At the onset of the project it was apparent that the spatial distribution of the boreholes throughout Salt Lake Valley (Figure 4) was not sufficiently uniform to allow an ArcGIS® algorithm to simply contour the predicted values of D_H and define the lateral spread hazard zones. Therefore, the mapped geologic units (Figure 1) became the primary delineation of the hazard zones and the lateral spread calculations of the borehole data within each unit was used to assign the level of hazard to each unit.

To begin this process, each borehole was assigned to its respective geologic unit using the available mapping (Figure 1). However, in some locations, relatively thin surficial geologic units are present and deeper boreholes penetrate layers found in underlying geologic units. Thus, during the data collection phase, it was important to assign each layer within each borehole to its respective geologic unit to account for variation in soil properties with depth. The classification of the layers in the borehole data by geologic unit made the subsequent statistical analysis more discriminating because the D_H values could be grouped and evaluated according to geologic unit, thus reducing the potential for miss-stratification and the potential additional variability it may produce. The Bartlett-Youd regression model (Bartlett and Youd, 1992; Youd et al., 2002) was used to calculate the distribution of D_H values within each geologic unit using the borehole data. The model is subdivided into an equation for a situation with a free-face nearby (Equation 1) and an equation for the situation of gently sloping terrain (Equation 2). The equations are as follows:

$$\log D_H = -16.713 + 1.532M - 1.406 \log R^* - 0.012R + 0.592 \log W + 0.540 \log T_{15} + 3.413 \log (100 - F_{15}) - 0.795 \log (D50_{15} + 0.1 \text{ mm}) \quad (1)$$

$$\log D_H = -16.213 + 1.532M - 1.406 \log R^* - 0.012R + 0.338 \log S + 0.540 \log T_{15} + 3.413 \log (100 - F_{15}) - 0.795 \log (D50_{15} + 0.1 \text{ mm}) \quad (2)$$

where: D_H is the amount of lateral spread predicted in meters,

M is the moment magnitude of earthquake anticipated,

R^* is a function of the horizontal distance to the fault given by:

$$R^* = R_0 + R \quad (3)$$

$$\text{where: } R_0 = 10^{(0.89*M - 5.64)} \quad (4)$$

R is the horizontal distance to the fault (km),

W is the ratio (%) of the height (H) of and the distance (L) to the free face,

S is the ground slope in percent as defined by Bartlett and Youd (1992)

T_{15} is the thickness (m) of the spreadable layer with $(N_1)_{60}$ less than 15,

F_{15} is the average fines content (%) of the spreadable layer, and

$D50_{15}$ is the average mean grain size (D_{50}) in the layer (mm).

This method was originally developed to estimate D_H for site-specific analyses, but because of the abundant geotechnical data compiled for Salt Lake County, it was possible to generalize this method and produce a regional hazard map. The potential for lateral spread was considered in all saturated, cohesionless layers having corrected Standard Penetration Test (SPT) $(N_1)_{60}$ blow count values (Youd et al., 2001) less than 15. Measurable lateral spread displacement is generally restricted to layers with $(N_1)_{60}$ values less than 15 for moderate to large earthquakes (M < 8.0). (However for very large earthquakes, e.g. M > 8.0, saturated cohesionless layers with $(N_1)_{60}$ values up to 20 may need to be evaluated for lateral spread (Bartlett and Youd, 1992). Layers that did not meet these criteria were screened from the analyses. Also, layers deeper than 15 m were not considered; such layers generally do not generate significant lateral spread displacement (Bartlett and Youd, 1992).

The analysis was implemented through a series of ArcGIS® routines to calculate the necessary parameters. To calculate R, an ArcGIS® geometry routine was developed to calculate the horizontal distance (km) from the borehole to the nearest point on the fault line (Figure 1) to be consistent with the definition of R used by Youd et al. (2002).

The ground slope, or the distance and height of a nearby free face, if present, greatly affect lateral spread displacement (Bartlett and Youd, 1992; Youd et al. 2002). A slope finder routine developed using ArcGIS® calculates the slope based on the position of the borehole relative to the toe and crest of the slope (Bartlett and Youd, 1992). For this routine to function, a Digital Elevation Model (DEM) was obtained from the USGS national elevation dataset and re-projected to coincide with the borehole coordinates. In essence, the slope finder routine searched a 200-m radius on the DEM grid from the borehole location and calculated the slope between every grid point within that radius so that the crests and toes of

influencing slopes nearby are found and their influence accounted for in the slope parameter to be consistent with the methodology of Bartlett and Youd (1992).

Another ArcGIS® routine was developed to calculate the free face ratio, W (%). To calculate W, location and depth of free face features such as river channels and canals were obtained for the mapped area in the form of an ArcGIS® line feature class. The routine then calculates the horizontal distance (L) from the borehole location to the closest free face feature in the ArcGIS® database. The height, or depth of the channel, (H) was also obtained from the feature database and W (%) was calculated for all boreholes. For cases where both a ground slope (S) and free face (W) were present, estimates of D_H were made for both cases and the larger estimate from the regression model was used to produce the map.

Lastly, the soil factors T_{15}, F_{15} and $D50_{15}$ were calculated for each borehole. These factors are the aggregated thickness (m) of saturated cohesionless sediments having $(N_1)_{60}$ values less than 15 and the corresponding average fines content and mean grain size for those layers. From these, values of D_H were calculated and plotted at each borehole location to inspect the variation and trends of D_H within a given surficial geologic unit. If a trend in D_H was noted (e.g., values of D_H generally increasing or decreasing in a certain area or direction within the unit), then this unit was subdivided during the hazard delineation to account for the differences or trends.

The hazard level was assigned to each geologic unit using statistical analysis of their D_H values. A cumulative histogram of the percentage of D_H values not exceeding the various hazard levels was plotted for each geologic unit. For example, Figure 7 shows the cumulative non-exceedance histogram for the hazard bins for the Qal_1 unit. For the low hazard bin (i.e., $0.0 < D_H < 0.1$ m), 50 percent of the data do not exceed the upper D_H limit for this bin (i.e., do not exceed 0.1 m). Also, for this unit, 71 percent of the data do not exceed the upper D_H limit for the high hazard bin (i.e., do not exceed 1.0 m). However, this also means that 29 percent of the predicted D_H values exceed 1.0 m, or are found in the very high hazard bin for this unit, which is still a significant percentage of the distribution. Thus, this remaining 29 percent might still justify this unit receiving a very high hazard ranking.

In consultation with our advisory board, we decided to use an 85 percent non-exceedance (15 percent exceedance) threshold to assign the hazard level to each geologic unit. This somewhat conservative threshold was chosen because it also approximates a mean plus one standard deviation threshold. In terms of exceedance, this threshold also means that no more than 15 percent of the estimated D_H values in a given unit can exceed a hazard

level's upper displacement range for the unit to be assigned to that hazard level. For example, in the case of Figure 7, 29 percent of the D_H values exceed 1.0 m (i.e., are greater than the high hazard bin); thus, this unit does not meet the above criterion for the high hazard level. Therefore, this unit would be assigned to the next highest hazard level where the criterion is true (e.g., very high hazard). Similarly, Figure 8 shows the cumulative non-exceedance histogram for the Qlaly and Qly units on the west side of Salt Lake Valley. In this case, 19 percent of the D_H values exceed the low hazard upper limit; thus this unit does not meet the criterion for this level. The unit was assigned to the moderate hazard level, where 0 percent of the data exceed the upper limit for this bin. This process of hazard level categorization was applied to all of the mapped units to produce the final map shown in Figure 6. In the event that a non-surficial geologic unit controlled the lateral spread hazard in a particular region, the hazard for the unit was subdivided to account for the underlying geologic unit and the boreholes in that region were analyzed separately according to the geologic unit.

The 85 percent non-exceedance criterion was selected because we believe that the end use of these maps warrants some conservatism in assigning a hazard level. In the past, Salt Lake County has used liquefaction triggering maps like that of Anderson et al. (1986) to delineate areas requiring site-specific geotechnical evaluations before land development is granted. Certainly, if our map is to be used for a similar purpose, then some conservatism is warranted in selecting the non-exceedance probability. (Other end-users and jurisdictions may select a different non-exceedance threshold, according to the end use of the map, but the proposed mapping method can still be applied.) We also recommend that site-specific geotechnical evaluations be considered for all areas with a moderate, or higher, lateral spread displacement hazard.

CONCLUSIONS

The lateral spread displacement hazard map shown in Figure 6 is the first of its type published for Salt Lake Valley. It uses site-specific geotechnical data correlated with surficial geologic units to define the potential lateral spread displacement hazard for a M7.0 scenario earthquake on the Salt Lake City segment of the Wasatch fault using peak horizontal ground acceleration estimates from Wong et al. (2002) for liquefaction triggering analyses. The lateral spread displacement hazard zones shown in Figure 6 are based on best estimates of horizontal ground displacement calculated from the Youd et al. (2002) lateral spread

regression equation. The amount of lateral spread displacements at each borehole location were categorized as follows: very high hazard (D_H > 1 m), high hazard (0.3 m < $D_H \leq$ 1.0 m), moderate hazard (0.1 m < $D_H \leq$ 0.3 m), low hazard (0.0 m < $D_H \leq$ 0.1 m) and minimal hazard (D_H = 0 m). Cumulative distribution histograms of D_H were calculated for each geologic unit and the above hazard categories assigned using an 85 percent non-exceedance probability threshold.

The lateral spread hazard zones shown in Figure 6 are based on estimates of horizontal displacement; thus this map delineates zones of potential building damage resulting from lateral spread. Previous liquefaction hazard mapping of Salt Lake Valley has focused on liquefaction susceptibility and potential (e.g., Figure 3), but such maps have not inherently considered lateral spread damage. We believe that lateral spread displacement maps can be used in conjunction with liquefaction potential maps to better characterize the amount and extent of lateral spread damage. In addition, Figure 6 has been developed from a more extensive subsurface database and updated geologic mapping, which improves its reliability. For example, most geologic units in the study area have several boreholes to characterize the pertinent soil properties and their variability. This larger sampling made it possible to develop cumulative distribution histograms of D_H for each unit (e.g., Figures 7 and 8). These histograms provide insight regarding the stochastic variability of lateral spread displacement within each unit and can also be used with probabilistic methods. Histograms for all geological units are presented in Bartlett and Olsen (2005).

The liquefaction hazard mapping efforts in Utah will continue in future years by mapping the lateral spread hazard for the southern half of Salt Lake Valley. Also, the project team plans to develop probabilistic liquefaction triggering, lateral spread displacement and liquefaction-induced ground settlement hazard maps for Salt Lake, Davis, Weber, Utah and Cache Counties. The hazard calculations for these maps will be coupled with probabilistic strong motion maps produced by the USGS to calculate the mean annual hazard of liquefaction and lateral spread and the best estimate of ground settlement for the mapped units. These probabilistic maps will be valuable tools for seismic risk assessment, loss estimation, urban planning and site remediation.

ACKNOWLEDGEMENTS

This effort is part of an ongoing USGS National Earthquake Hazards Reduction Program mapping project for Utah (NEHRP Award 04HQGR0026). The Utah Liquefaction Advisory Group (ULAG) recommends priorities for NEHRP-funded liquefaction studies in Utah. We thank the USGS for the funding of this research and ULAG for its participation in guiding and reviewing this work.

REFERENCES

Anderson, L.R., Keaton, J.R., Aubry, K., and Ellis, S.J., (1982). *Liquefaction potential map for Davis County, Utah, Final Report to the U.S. Geological Survey*.

Anderson, L. R., Keaton, J. R., Spitzley, J. E., and Allen A. C., 1986. *Liquefaction potential map for Salt Lake County, Utah: Utah State University Department of Civil and Environmental Engineering and Dames and Moore, unpublished final technical report prepared for the U.S. Geological Survey,* National Earthquake Hazards Reduction Program Award No. 14-08-0001-19910, 48 p; published as Utah Geological Survey Contract Report 94-9, 1994.

Ashland, F. X., and McDonald, G. N., 2003. *Interim map showing shear wave velocity characteristics of engineering geological units in the Salt Lake Valley, Utah metropolitan area: Utah Geological Survey Open File Report 424*, 43 p. pamphlet, scale 1:75,000, CD-ROM.

Bartlett S. F., Olsen, M. J., and Solomon, B. J., 2005, *Lateral Spread Hazard Mapping of Northern Salt Lake County for a Magnitude 7.0 Scenario Earthquake*, Technical Report submitted to the United States Geological Survey, NERHP Award No. 04HQGR0026, 218 p.

Bartlett, S. F., and Youd T. L., 1992. *Empirical analysis of horizontal ground displacement generated by liquefaction-induced lateral spreads*, Technical Report NCEER-92-0021, National Center for Earthquake Engineering Research, Buffalo, NY.

Biek, R.F., Solomon, B.J., Keith, J.D., and Smith, T.W., 2004. *Interim geologic maps of the Copperton, Magna, and Tickville Spring quadrangles, Salt Lake and Utah Counties, Utah: Utah Geological Survey Open-File Report 434*, scale 1:24,000.

Boulanger, R. W., and Idriss, I.M., 2004. *Evaluating the potential for liquefaction or cyclic failure of silts and clays*, Technical Report UCD/CGM-04/01, Center for Geotechnical Modeling, University of California at Davis.

Hamada, M., Yasuda, S., Isoyama, R., and Emoto, I., 1986. *Study on liquefaction induced permanent ground displacements*, Report for the Association for the Development of Earthquake Prediction.

Iwasaki, T., Tatsuoka, F., Tokida, K. and Yasuda, S., 1978. *A practical method for assessing soil liquefaction potential based on case studies at various sites in Japan*, Proc, 2nd Int. Conf. On Microzontation, San Francisco, California, p. 885-896.

Jarva, J.L., 1994. *Liquefaction-potential map for a part of Salt Lake County, Utah*, Utah Geological Survey Public Information Series 25, scale 1:300,000.

Kleinfelder Inc., 1999. *Geological investigation, proposed Salt Palace Expansion II, Salt Lake City, Utah*, prepared by Kleinfelder Associates, Feb. 26, 1999.

Lund, W. R., 2005. *Consensus preferred recurrence-interval and vertical slip-rate estimates*, Utah Geological Survey Bulletin 134, CD-ROM

Miller, R.D., 1980. *Surficial geologic map along part of the Wasatch Front, Salt Lake Valley, Utah*, U.S. Geological Survey Miscellaneous Field Studies Map MF-1198, scale 1:100,000.

NCEER, 1997. *Proceedings of the NCEER workshop on evaluation of liquefaction resistance of soils*, Technical Report NCEER-97-0022, National Center for Earthquake Engineering Research, Buffalo, New York.

O'Rourke, T.D., and Pease, J.W., 1997. *Mapping liquefiable layer thickness for seismic hazard assessment*. Journal of Geotechnical and Geoenvironmental Engineering, American Society of Civil Engineers, Vol. 123, No. 1, January, p. 46-56.

Osmond, J. C., Hewitt, W. P., and Van Horn, R. V., 1965. *Engineering implications and geology, Hall of Justice excavation*, *Salt Lake City, Utah*, Utah Geological and Mineral Survey Special Studies No. 11, 35 p.

Oviatt, C.G., Currey, D.R., and Sack, D., 1992. *Radiocarbon chronology of Lake Bonneville, eastern Great Basin, U.S.A*., Palaeogeography, Palaeoclimatology, and Palaeoecology, Vol. 99, p. 225-241

Personius, S.F., and Scott, W.E., 1992. *Surficial geologic map of the Salt Lake City segment and parts of adjacent segments of the Wasatch fault zone*, Davis, Salt Lake, and Utah Counties, Utah: U.S. Geological Survey Miscellaneous Investigations Map I-2106, scale 1:50,000.

Rosinski, A., Knudsen, K.L., Wu, J., Seed, R.B., Real, C.R., 2004. *Development of regional liquefaction-induced deformation hazard maps*, GeoTrans 2004, Geotechnical Engineering for Transportation Projects (GSP No. 126), ASCE Conf. Proc. Vol. 154, No. 67, p. 797-806.

Simon, D. and Bymaster, W., 1999. *Report of geologic investigation, Salt Palace Convention Center Expansion Project*, *100 South West Temple Street, Salt Lake City, Utah*, prepared by SBI Geotechnical and Environmental Engineering, March 29, 1999.

Smith, R.B., and Arabasz, W.J., 1991. *Seismicity of the intermountain seismic belt, Neotectonics of North America*, Geological Society of North America, SMV V-1, p. 185-228.

Toprak, S. and Holzer, T. L., 2003. *Liquefaction Potential Index: Field Assessment*, Journal of Geotechnical and Geoenvironmental Engineering, American Society of Civil Engineers, Vol. 129, No. 4, p. 315-322.

Wong, I., Silva, W., Wright, D., Olig, S., Ashland, F., Gregor, N., Christenson, G., Pechmann, J., Thomas, P., Dober, M., and Gerth, R., 2002. *Ground-shaking map for a magnitude 7.0 earthquake on the Wasatch fault, Salt Lake City, Utah, metropolitan area*, Utah Geologcial Survey Miscellaneous Publication MP 02-05, 50 p., Utah Geological Survey Public Information Series 76.

Youd, T. L., and Perkins, D. M., 1978. *Mapping liquefaction-induced ground failure potential*, Journal of the Geotechnical Engineering Division, ASCE, Vol. 104, No. GT4, Proc Paper 13659, April, 1978, p. 433-446.

Youd, T.L., and Perkins, D.M., 1987. *Mapping of liquefaction severity index*, Journal of Geotechnical Engineering Division, American Society of Civil Engineers, Vol. 118, p. 1374-1392.

Youd, T.L., and Idriss, I.M., Andrus, R.D. Arango, I., Castro, G., Christian, J.T., Dobry, R., Liam Finn, W.D.L., Harder, L.F., Jr., Hynes, M.E., Ishihara, K., Koester, J.P., Liao, S.S.C., Marcuson, W.F., III, Martin, G.R., Mitchell, J.K., Moriwaki, Y., Power, M.S., Robertson, P.K., Seed, R.B., and Stokoe, K.H., II, 2001. *Liquefaction resistance of soils: Summary report from the 1996 NCEER and 1998 NCEER/NSF workshops on evaluation of liquefaction resistance of soils*, J. Geotech. Geoenviron. Eng., Vol. 127, No. 10, p. 817-833.

Youd, T.L., Hansen, C.M., and Bartlett S.F., 2002. *Revised multilinear regression equations for prediction of lateral spread displacement*, Journal of Geotechnical and Geoenvironmental Engineering, Vol. 128, No. 12, p. 1007-1017.

Table 1. Geologic units and descriptions

Name	Description	Age	# SPT
Stream Alluvium			
Qal_1	Modern stream alluvium 1	Upper Holocene	136
Qal_2	Modern stream alluvium 2	Upper Holocene	59
Qalp	Stream alluvium related to the Provo (regressive) Phase of Lake Boneeville	Upper Pleistocene	10
Qaly	Stream alluvial deposits, undivided	Holocene - Upper Pleistocene	16
Alluvial Fan Deposits			
Qaf_2	Alluvial-fan deposits 2	Holocene	23
Qafy	Alluvial-fan deposits, undivided	Holocene - Upper Pleistocene	6
Young Lacustrine and Mixed-Environment Deposits			
Qly	Lacustrine and marsh deposits	Holocene	15
Qlaly	Lacustrine, marsh, and alluvial deposits	Holocene – Upper Pleistocene	102
Lake Bonneville Lacustrine Deposits			
Qlpg	Lac. gravel and sand of the Provo (regressive) phase	Upper Pleistocene	13
Qlps	Lac. sand and silt of the Provo (regressive) phase	Upper Pleistocene	5
Qlpm	Lac. clay and silt of the Provo (regressive) phase	Upper Pleistocene	3
Qlbg	Lac. gravel and sand of the Bonneville (transgressive) phase	Upper Pleistocene	9
Qlbs	Lac. sand and silt of the Bonneville (transgressive) phase	Upper Pleistocene	1
Qlbm	Lac. clay and silt of the Bonneville (transgressive) phase	Upper Pleistocene	3
Qlbpg	Lac. gravel and sand of the Bonneville Lake cycle, undivided	Upper Pleistocene	9
Qlbps	Lac. sand and silt of the Bonneville Lake cycle, undivided	Upper Pleistocene	3
Qlbpm	Lac. silt and clay of the Bonneville Lake cycle, undivided	Upper Pleistocene	198
Colluvial Deposits			
Qclsp	Lateral spread deposits	Holocene – Upper Pleistocene	1
Qca	Colluvium and alluvium, undivided	Holocene – Middle Pleistocene.	1
Artificial Deposits			
Qf	Artificial fill	Historical	4
Bedrock*			
Tn	Tertiary sedimentary and volcanic rocks	Neogene	0
Tp	Tertiary sedimentary and volcanic rocks	Paleogene	0
Mz	Mesozoic sedimentary rocks	Cretaceous – Triassic	0
Pz	Paleozoic sedimentary rocks	Permian – Cambrian	0
pC	Precambrian metamorphic rocks	Proterozoic and Archean	0

*There are no data available in these units, however, they are non-liquefiable deposits (very dense and deep groundwater table)

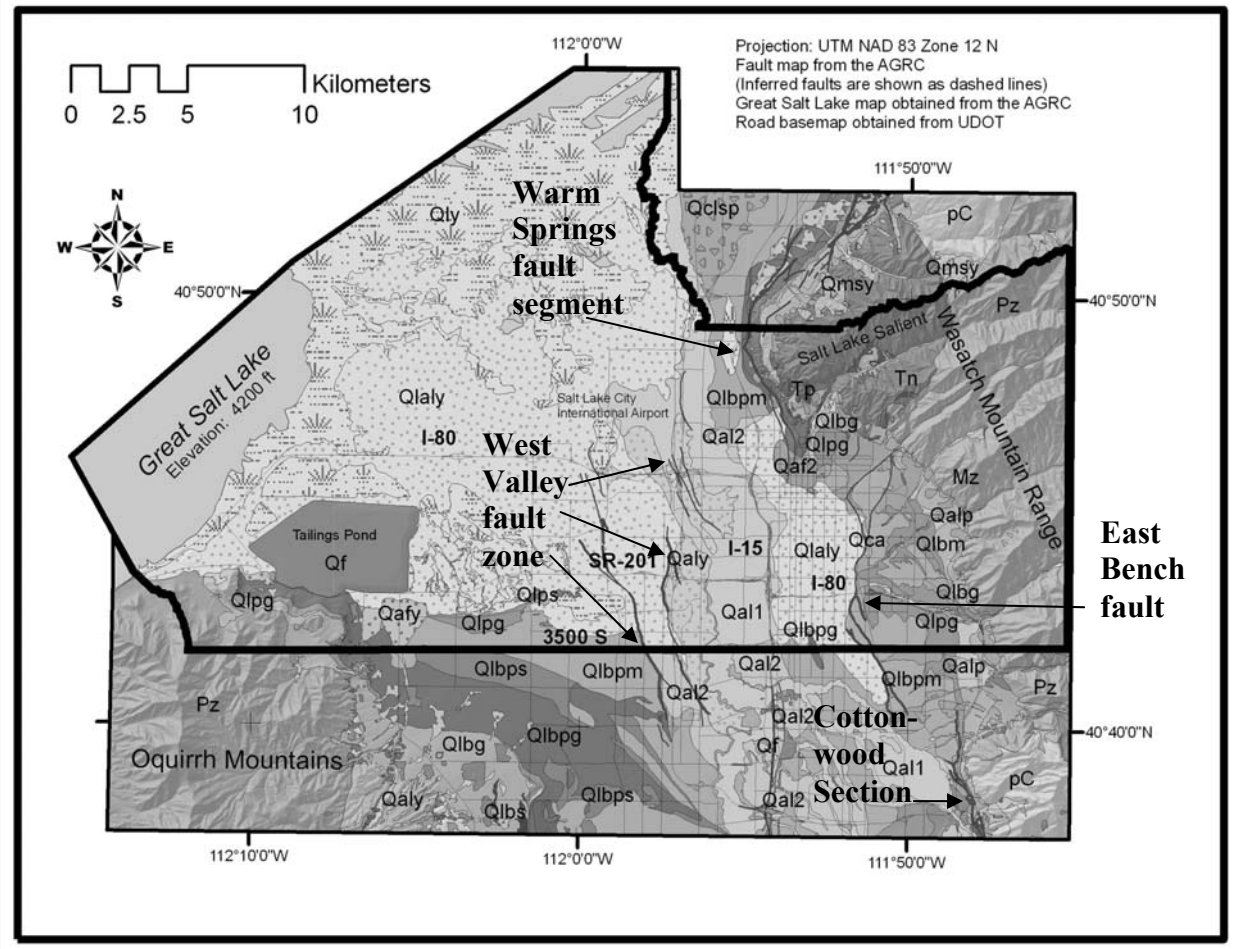

Figure 1. Study area (outlined in black) and surficial geology of northern Salt Lake County, Utah (modified from Personius and Scott (1992), Biek et al. (2004) and Miller (1980)) (See Table 1 for description of geologic units).

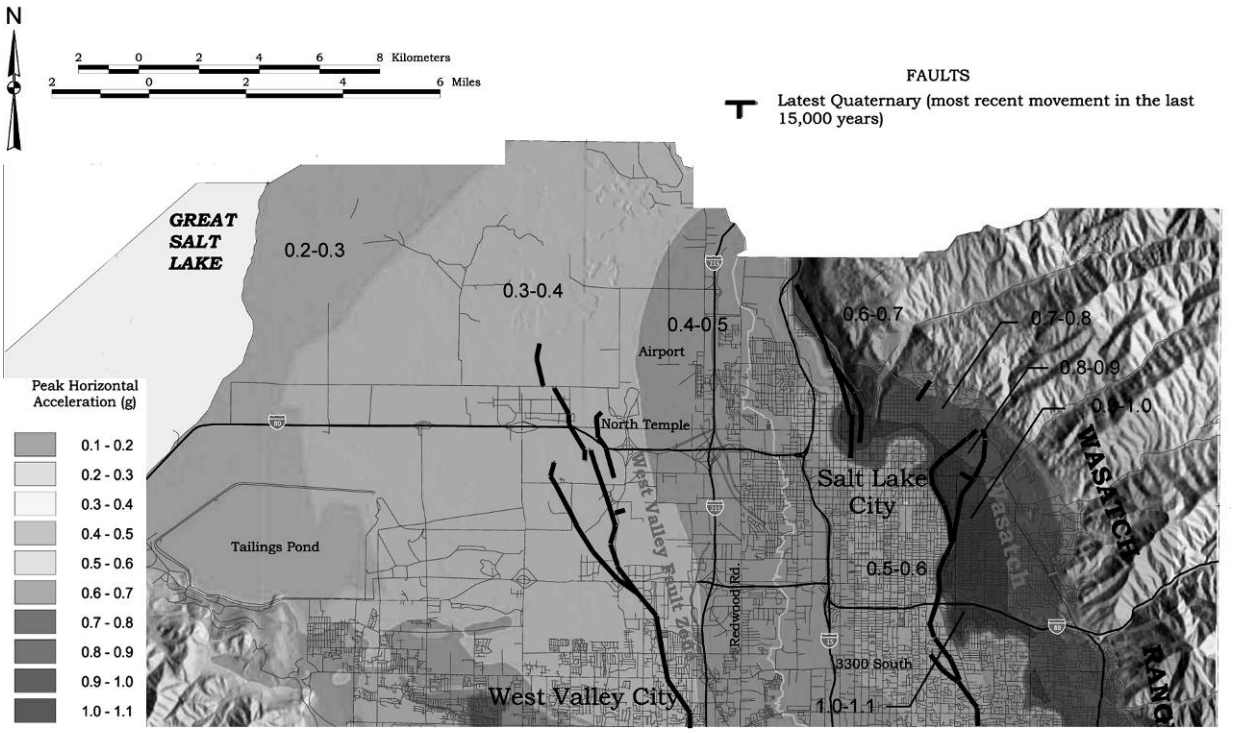

Figure 2. Estimates of the peak horizontal ground acceleration (pga) for northern Salt Lake Valley, Utah for a M7.0 scenario earthquake from Wong et al. (2002).

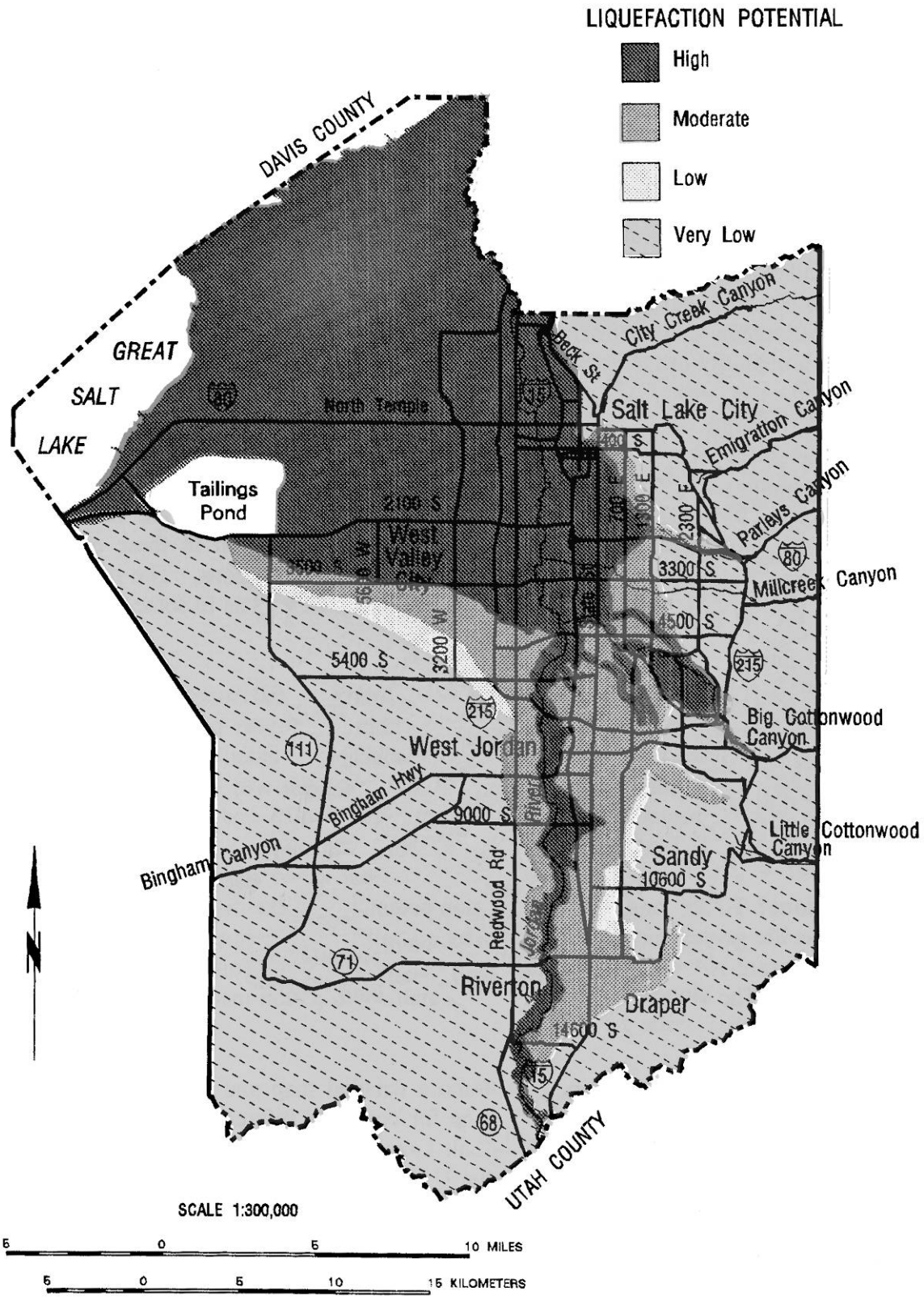

Figure 3. Liquefaction potential map for Salt Lake Valley, Utah (Jarva 1994, modified from Anderson et al. 1986).

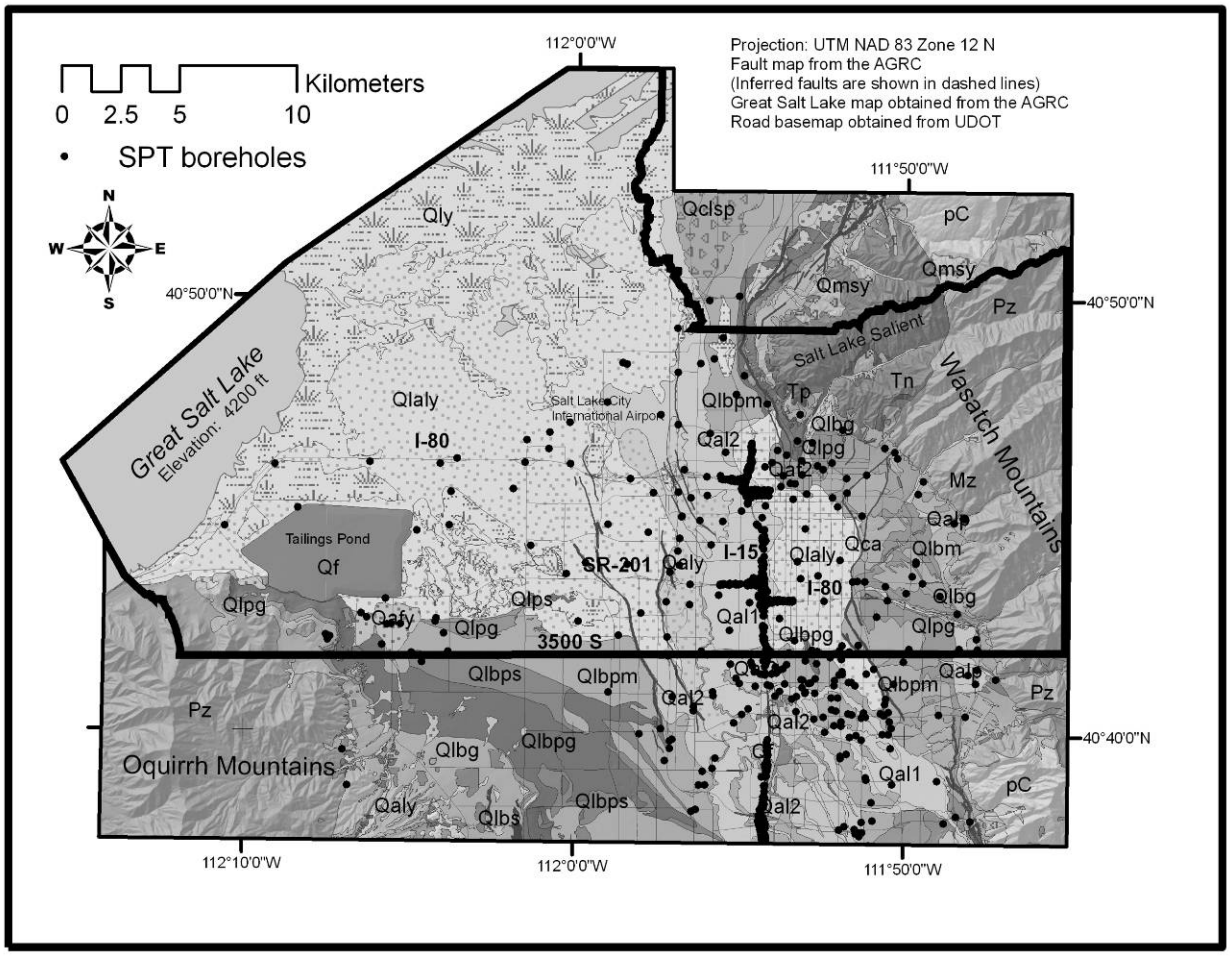

Figure 4. Standard Penetration Test (SPT) locations entered into ArcGIS® database for northern Salt Lake Valley, Utah.

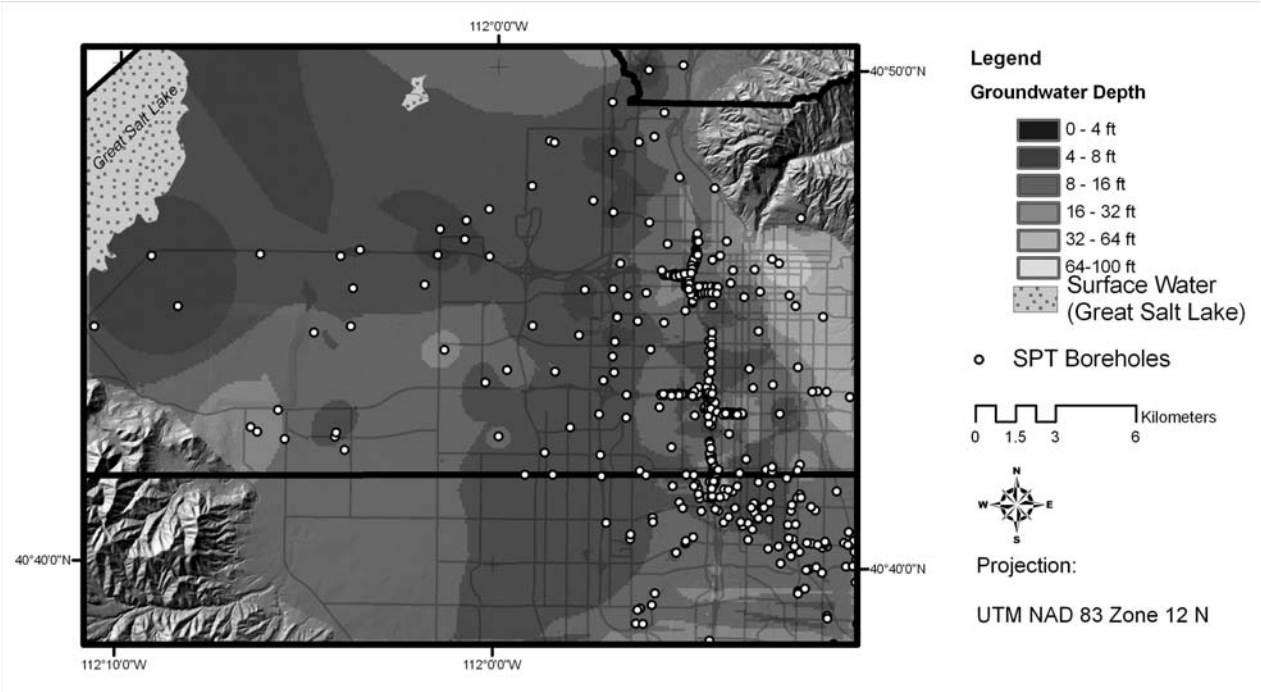

Figure 5. Depth to groundwater map for northern Salt Lake Valley, Utah using inverse distance squared interpolation of geotechnical borehole data.

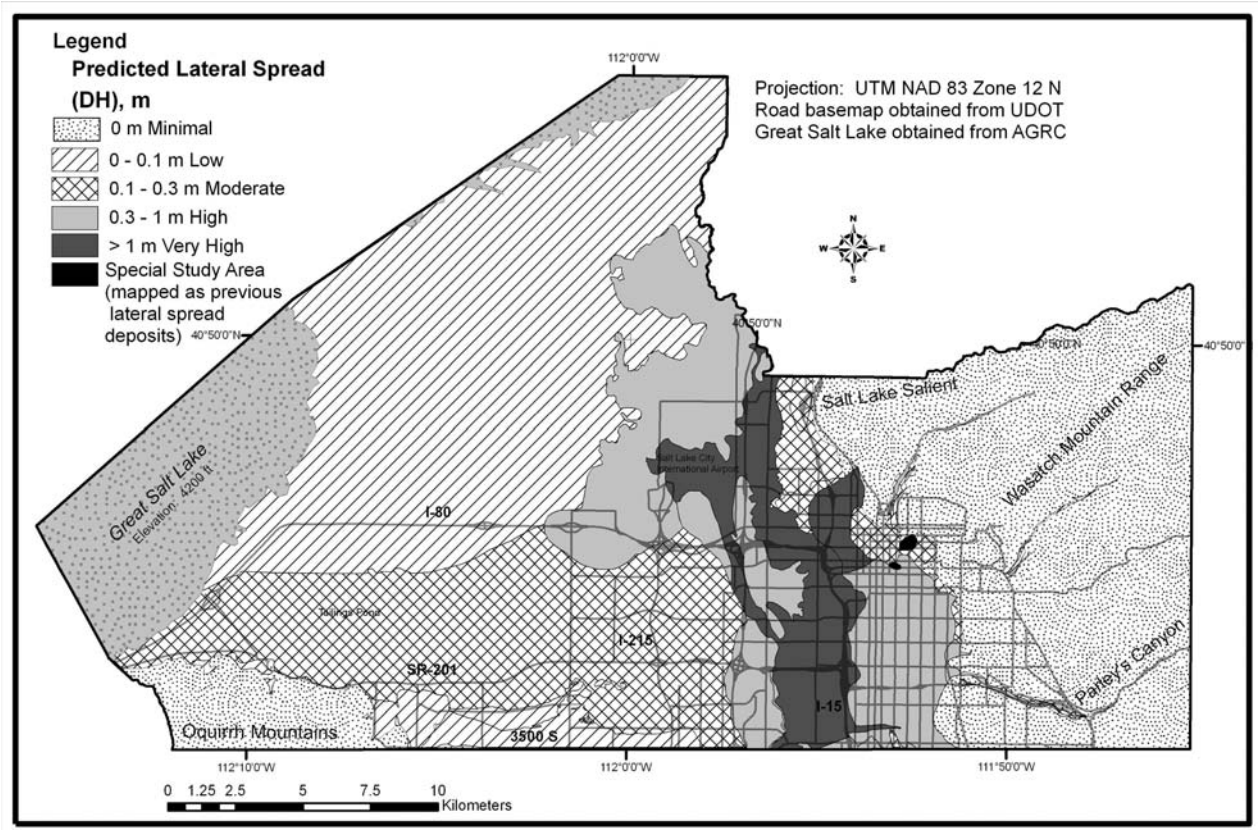

Figure 6. Lateral spread hazard map for northern Salt Lake Valley, Utah.

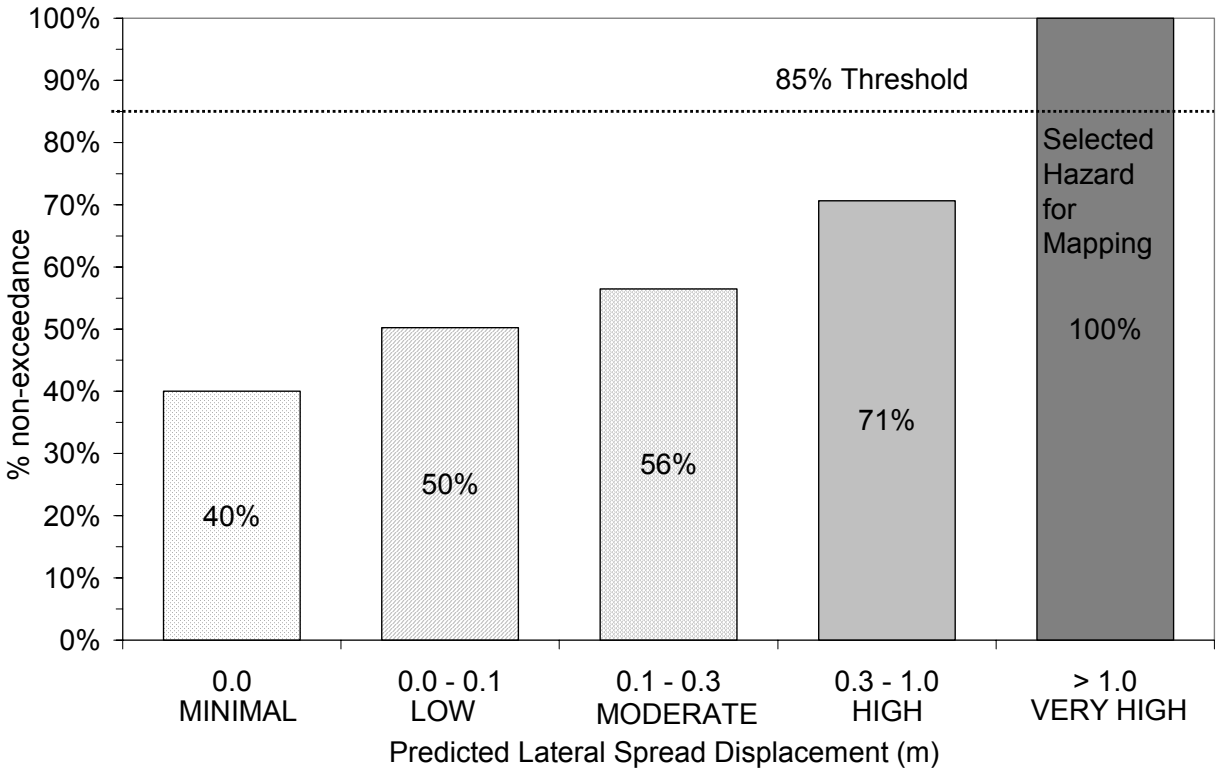

Figure 7. Cumulative histogram of non-exceedance percentages of D_H values for the Qal_1 unit.

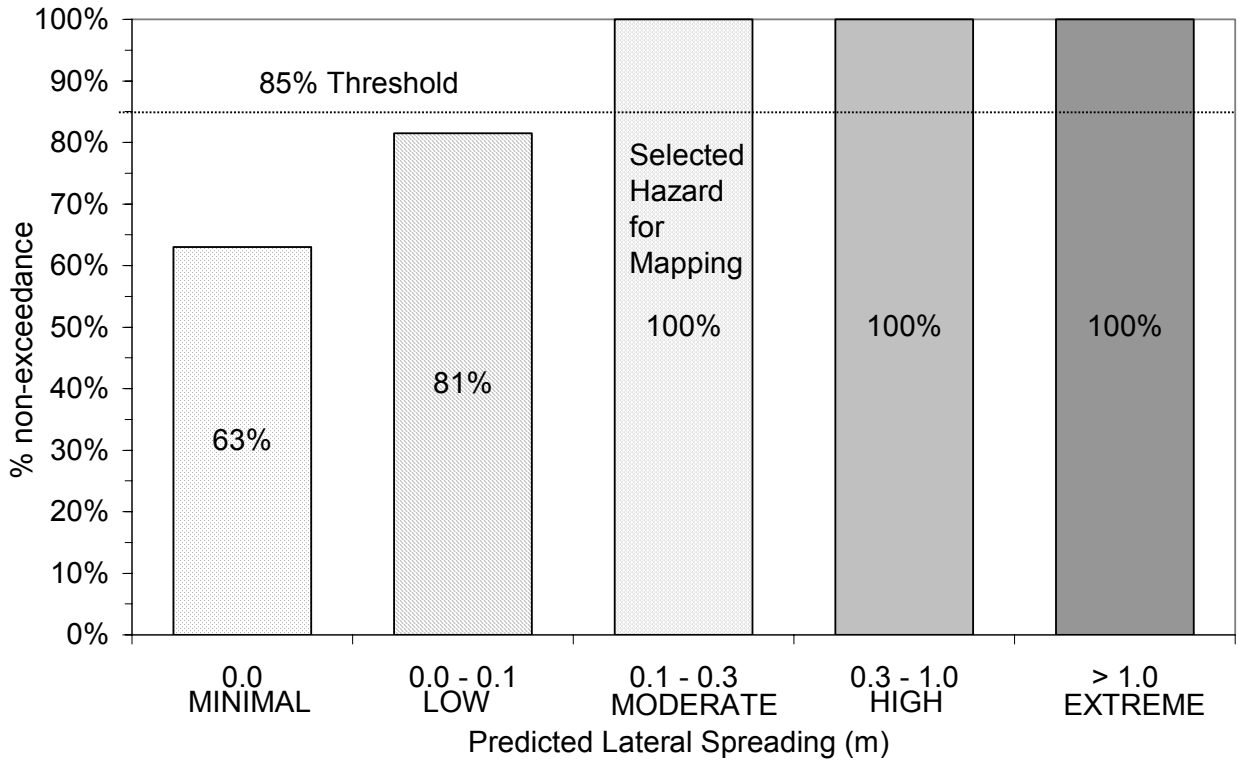

Figure 8. Cumulative histogram of non-exceedance percentages of D_H values for the Qlaly and Qly units on the west side of Salt Lake Valley.